



The Dynamic Covalent Chemistry of Amidoboronates: Tuning the rac_5/rac_6 Ratio via the B–N and B–O Dynamic Covalent Bonds

Patrick Harders,^[a] Thomas Griebenow,^[a] Artjom Businski,^[a] Anton J. Kaus,^[a] Lorenz Pietsch,^[a] Christian Näther,^[b] and Anna J. McConnell^{*[a]}

Amidoboronates were prepared as a mixture of up to three isomers (rac_5 , $meso_5$ and rac_6) from the reductive coupling of *N*-aryl iminoboronates with either cobaltocene or decamethylcobaltocene in acetonitrile. The interconversion of rac_5 and rac_6 isomers via rearrangement of their dynamic covalent B–N bonds was investigated in solution by redissolving isolated crystals. The aniline *para* substituent and catechol within the amidoboronates tuned the rac_5/rac_6 ratio; the rac_6 isomer predominated for amidoboronates based on pyrocatechol,

ranging from a ratio of 0:1 with electron-withdrawing Cl substituents to 0.5:0.5 for electron-donating NMe₂ substituents. No interconversion was observed for the rac_5 isomers of amidoboronates based on tetrachlorocatechol. Furthermore, the rac_5/rac_6 distribution was altered by catechol exchange of pyrocatechol for tetrachlorocatechol exploiting the dynamic covalent B–O bonds and the rac_5 isomer was the major isomer following exchange.

Introduction

BN-containing compounds and materials such as B–N heterocycles,^[1] frustrated Lewis pairs (FLPs)^[2] and polyaminoboranes^[3] have gained attention since different reactivity and functionality can be accessed compared to their carbon analogues through the polarity of the B–N bond as well as the ability of boron and nitrogen to form not only covalent but also coordinative bonds.^[1a,b] In materials science this has been exploited to tune the optoelectronic^[1d,f,i,k,4] and self-healing^[5] properties of materials. Furthermore, amidation reactions have been catalysed by BN-containing heterocycles,^[1e,6] and FLPs^[2,7] enable small molecule activation (e.g. H₂, CO₂) and catalysis as an alternative to transition metal catalysts.

Dynamic covalent chemistry^[8] exploits the reversibility of bond-breaking and formation for a variety of applications from the self-assembly of supramolecular architectures^[9] to bioconjugation,^[10] and the development of self-healing

polymers,^[11] malleable thermoset materials^[12] and gels.^[10a,13] Dynamic covalent bonds include disulfides,^[9e,f,14] C–O bonds^[8d] (e.g. esters,^[15] acetals^[16] and orthoesters^[9a,b]), Si–O bonds,^[17] C=N bonds (e.g. hydrazones,^[14c,18] imines^[9g,i,m,19]) and B–O bonds (e.g. boronate esters,^[9h,j,k,10a,14c,20] boroxines^[5b,9l,12a,21]). Combining imine and boronate ester bonds, iminoboronates are self-assembled from an amine, 2-formylphenylboronic acid and a diol using dynamic covalent chemistry.^[8c,22] Given the dynamic nature of these two bonds, more electron-deficient anilines have been exchanged for more electron-rich anilines and aliphatic diols exchanged for catechols due to greater delocalisation of the partial negative charges on oxygen in the aromatic diol.^[22c]

Iminoboronates find application in determining the enantiopurity of amines and amino acids,^[20a,22b,23] self-healing polymers,^[21,24] bioconjugation,^[25] drug delivery^[26] and self-assembly.^[22c] We also recently exploited their reactivity in a reductive coupling with cobaltocene to access up to three amidoboronate products following C–C bond formation: the diastereomeric $meso_5$ and rac_5 products and the rac_6 product with a fused six-membered heterocyclic ring system formed from the rac_5 isomer via rearrangement of the covalent B–N bonds (Scheme 1).^[27]

We report the expanded scope of the reductive coupling in acetonitrile varying both the *para* substituent of the aniline and catechol to obtain single isomers of the rac_5 or rac_6 isomers via crystallisation. The rac_5/rac_6 interconversion and resulting isomeric ratio of the redissolved crystals was tuned by electronic effects via the B–N and B–O dynamic covalent bonds (Scheme 1). The rac_6 isomer predominated for amidoboronates based on pyrocatechol with electron-withdrawing aniline substituents but the amount of the rac_5 isomer increased as the electron donating ability of the aniline substituent increases. In contrast, amidoboronates based on tetrachlorocatechol crystal-

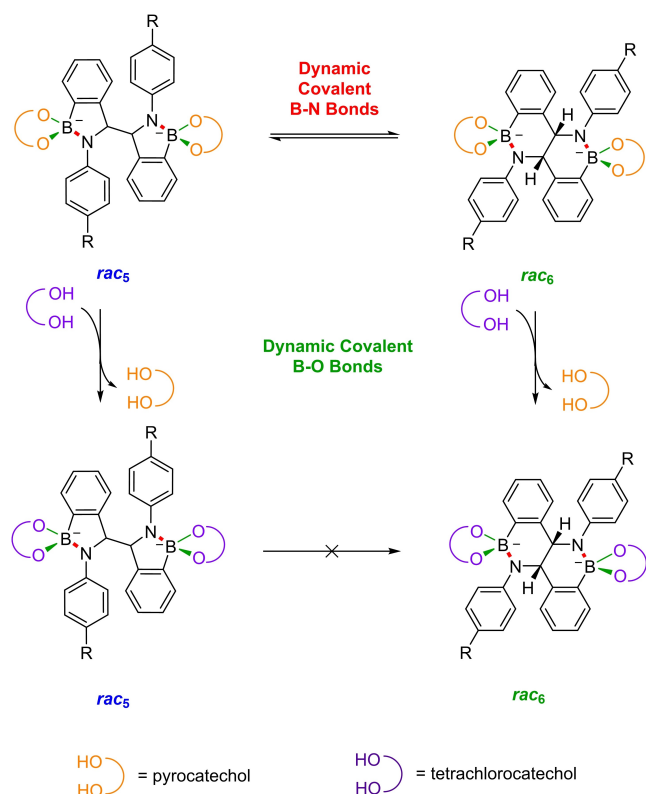
[a] P. Harders, T. Griebenow, A. Businski, A. J. Kaus, L. Pietsch, Prof. Dr. A. J. McConnell
Otto Diels Institute of Organic Chemistry
Christian-Albrechts-Universität zu Kiel
Otto-Hahn-Platz 4, 24098 Kiel (Germany)
E-mail: amcconnell@oc.uni.kiel.de

[b] Prof. Dr. C. Näther
Institute of Inorganic Chemistry
Christian-Albrechts-Universität zu Kiel
Max-Eyth-Straße 2, 24118 Kiel (Germany)

Supporting information for this article is available on the WWW under <https://doi.org/10.1002/cplu.202200022>

This article is part of a Special Collection celebrating the 10th Anniversary of ChemPlusChem.

© 2022 The Authors. ChemPlusChem published by Wiley-VCH GmbH. This is an open access article under the terms of the Creative Commons Attribution License, which permits use, distribution and reproduction in any medium, provided the original work is properly cited.



Scheme 1. Interconversion between the *rac*₅ and *rac*₆ amidoboronate isomers based on pyrocatechol via dynamic covalent B–N bonds (red) and catechol exchange of pyrocatechol for tetrachlorocatechol via dynamic covalent B–O bonds (green).

lised as the *rac*₅ isomer and no interconversion to the *rac*₆ isomer was observed. Finally, we demonstrate that the B–O bonds of the amidoboronates are dynamic and catechol exchange of pyrocatechol for tetrachlorocatechol alters the *rac*₅/*rac*₆ ratio with the *rac*₅ isomer predominating.

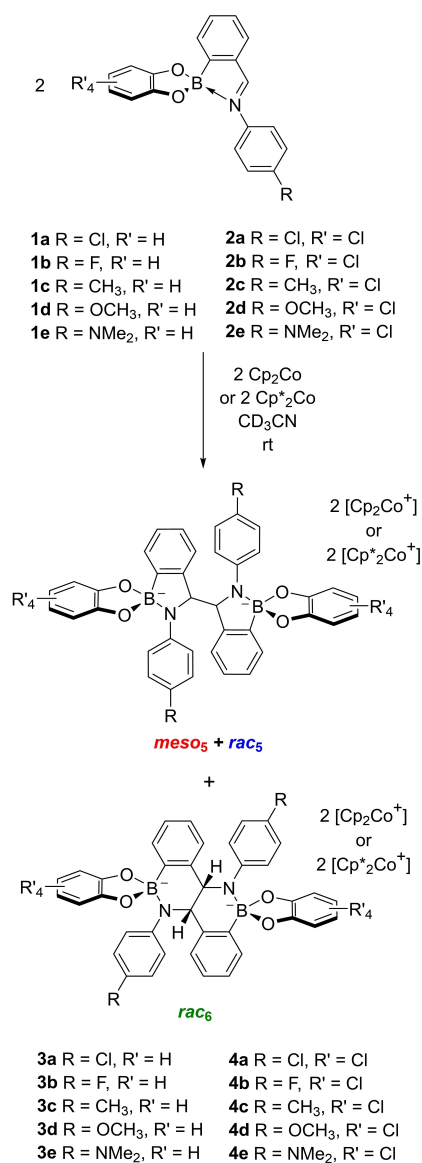
Results and Discussion

To investigate the influence of electronic effects on the dynamic covalent chemistry of the amidoboronate products from the reductive coupling, the aniline substituents (R) were varied from Cl (σ_p 0.23) to NMe₂ (σ_p –0.83) to cover a range of Hammett parameters^[28] and the catechol was varied from pyrocatechol (R' = H) to tetrachlorocatechol (R' = Cl). Of particular interest were the *rac*₅/*rac*₆ isomeric distribution following interconversion via the dynamic covalent B–N bonds and the dynamic nature of the B–O bonds since this could enable tuning of the *rac*₅/*rac*₆ ratio via catechol exchange.

The iminoboronate substrates **1a–e** and **2a–e** for the reductive coupling were prepared by mixing 2-formylphenylboronic acid, the appropriate 4-substituted aniline and catechol (pyrocatechol or tetrachlorocatechol) in a 1:1:1 ratio in acetonitrile (Schemes S1 and S2). Iminoboronates **1a–e** and **2c** have been reported previously.^[22c,27] X-ray crystal structures of **1a** (Figure S3), **1d** (Figure S4), **1e** (Figure S7) and **2d** (Fig-

ure S15) showed the iminoboronate structure with a dative bond between the imine nitrogen and tetrahedral boron centre.^[29] The B–N dative bond lengths (1.662–1.684 Å) were similar to those in related iminoboronates^[23a] and aminomethylboronate esters.^[20c]

The reductive couplings of **1a–1e** and **2a–2e** were carried out with cobaltocene or decamethylcobaltocene as the reductant in acetonitrile to obtain crystals of single isomers for studies on the dynamic covalent chemistry of the amidoboronate products (Scheme 2). We have previously reported the solid-state and solution structures of [*meso*-**3b**](Cp₂Co)₂, [*rac*₆-**3b–d**](Cp₂Co)₂ and [*rac*₅-**4c**](Cp⁺₂Co)₂,^[27] Decamethylcobaltocene was chosen as an alternative reductant in these studies to investigate: i) whether different amidoboronate isomers could be crystallised with decamethylcobaltocenium rather than



Scheme 2. Reductive coupling of *N*-aryl iminoboronates **1a–1e** and **2a–2e** with cobaltocene or decamethylcobaltocene giving up to three amidoboronate products (*meso*₅, *rac*₅ and *rac*₆).

cobaltocenium counteranions; ii) the influence of the counteranion on the *rac*₅/*rac*₆ rearrangement.

While the reductive couplings were monitored by NMR spectroscopy, conclusions about the *meso*₅/*rac*₅/*rac*₆ product distribution could not be made in many cases due to competing crystallisation from the reaction mixture. For example, the reductive coupling of iminoboronate **1e** with cobaltocene could not be monitored by NMR spectroscopy due to the speed of crystallisation and as a result of the low concentration left in solution (although there was no evidence of the *meso*₅ isomer). Despite numerous attempts, suitable crystals for X-ray analysis could not be obtained from this reductive coupling. Furthermore, crystallisation did not take place in the analogous reductive coupling with decamethylcobaltocene, although *rac*₅-**3e** was the predominant isomer in the reaction mixture (Figure S52). Crystals were also not obtained from the reductive couplings of **3a–3d** with decamethylcobaltocene.

Solid-state structures were obtained from crystals of [*meso*₅-**3a**](Cp₂Co)₂ (Figure 1a), [*rac*₆-**3a**](Cp₂Co)₂ (Figure 1b), [*rac*₅-**4a**](Cp^{*}₂Co)₂ (Figure S69), [*rac*₅-**4d**](Cp₂Co)₂ (Figure 1c), [*rac*₅-**4e**](Cp₂Co)₂ (Figure S124) and [*rac*₅-**4e**](Cp^{*}₂Co)₂ (Figure S130)^[29] and the corresponding solution structures were obtained by redissolving the crystals in DMSO-*d*₆ (SI, Sections 3.2.2, 3.3.2, 8.2.2, 11.2.2, 12.2.2, 12.3.2). While solid-state structures were not obtained of crystals from several reductive couplings, their solution structures were revealed to be [*rac*₅-**3e**](Cp₂Co)₂ and [*rac*₅-**4d**](Cp^{*}₂Co)₂ upon redissolving the crystals in DMSO-*d*₆ (SI, Sections 7.2.1, 11.3.1).

Carbon-centred radicals are known to dimerise to form thermodynamically stable *anti* and *gauche* conformations.^[30] All of the crystal structures show the *gauche* conformer with the exception of [*meso*₅-**3a**](Cp₂Co)₂ as the *anti* conformer (Figure 1a). Since [*meso*₅-**3a**](Cp₂Co)₂ was grown from a vapour diffusion crystallisation with toluene rather than directly from the acetonitrile reaction mixture like the other crystals, these crystallisation conditions could account for the difference in conformation.

Comparisons can be made on the amidoboronate products obtained by crystallisation from the series of reductive couplings varying the aniline *para* substituent, catechol and counteranion in this and the previous study.^[27] Within the pyrocatechol series (**3a–3e**), the *rac*₆ isomer crystallised from

the reaction mixtures as the cobaltocenium salt with the exception of [*rac*₅-**3e**](Cp₂Co)₂ with NMe₂ substituents (Figures S57–S62). Furthermore, crystals of [*meso*₅-**3a**](Cp₂Co)₂ (Figure 1a, S27–S31) and [*meso*₅-**3b**](Cp₂Co)₂^[27] with the electron-withdrawing Cl and F substituents, respectively, were obtained on separate occasions to the *rac*₆ isomer. In contrast, the *rac*₅ isomer crystallised for the tetrachlorocatechol series with cobaltocenium (**4c–4e**) and decamethylcobaltocenium counteranions (**4a, 4c–4e**).

Crystals of the *rac*₅ and *rac*₆ isomers were redissolved in DMSO-*d*₆ to not only characterise the single isomers in solution by NMR spectroscopy but also investigate the influence of the aniline *para* substituent, catechol and counteranion on the *rac*₅/*rac*₆ interconversion with a range of amidoboronates. Within the pyrocatechol series (Scheme 3a), *rac*₆-**3a**^[31] was not observed to interconvert to the *rac*₅ isomer even after 5 days and the *rac*₆ isomer remained the predominant isomer at equilibrium for **3c–d**^[32] (Figures 2a and S136). While **3e** with the most electron-rich NMe₂ substituent crystallised as the *rac*₅ isomer, a 1:1 mixture of the *rac*₅/*rac*₆ isomers was obtained at equilibrium.

Comparing the series of interconversions, the fraction of the two isomers at equilibrium appears to correlate with the Hammett parameter of the aniline *para* substituent (Figure 2a); there is a greater proportion of the *rac*₆ isomer at equilibrium with the most electron-withdrawing Cl-substituted amidoboronate and least with the most electron-donating NMe₂-substituted amidoboronate. The increased interconversion is attributed to the greater electron density on the nitrogen and boron centres, facilitating B–N bond cleavage.^[27] It was not possible to investigate the influence of the counteranion on the interconversion as crystals were not obtained from the reductive couplings with decamethylcobaltocene.

For the tetrachlorocatechol series (Scheme 3b), the redissolved *rac*₅-**4a**, *rac*₅-**4c**, *rac*₅-**4d** and *rac*₅-**4e** isomers were not observed to interconvert to the *rac*₆ isomer regardless of the counteranion (Cp₂Co⁺ or Cp^{*}₂Co⁺) before decomposition of the amidoboronates was observed over time (Figures 2b and S137–138). This lack of interconversion is attributed to strengthening of the B–N bond by reduction of the electron density around the boron and nitrogen centres due to the electron-withdrawing tetrachlorocatechol even in the presence

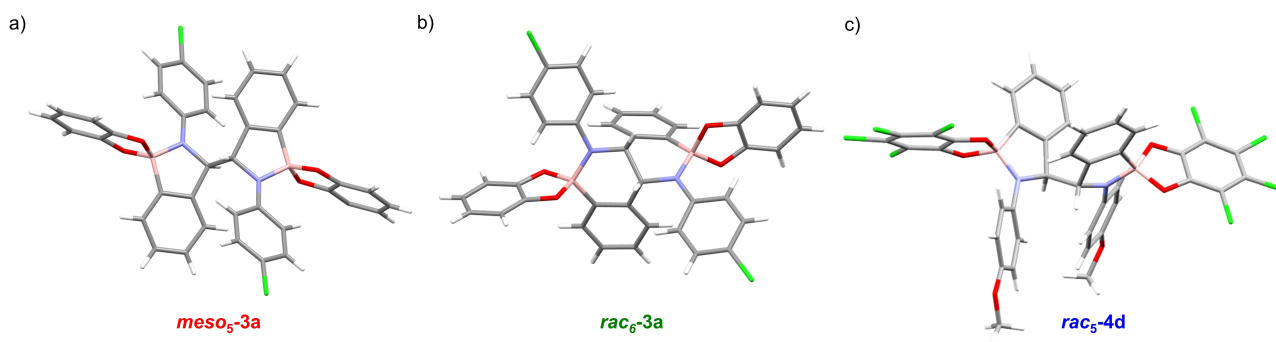
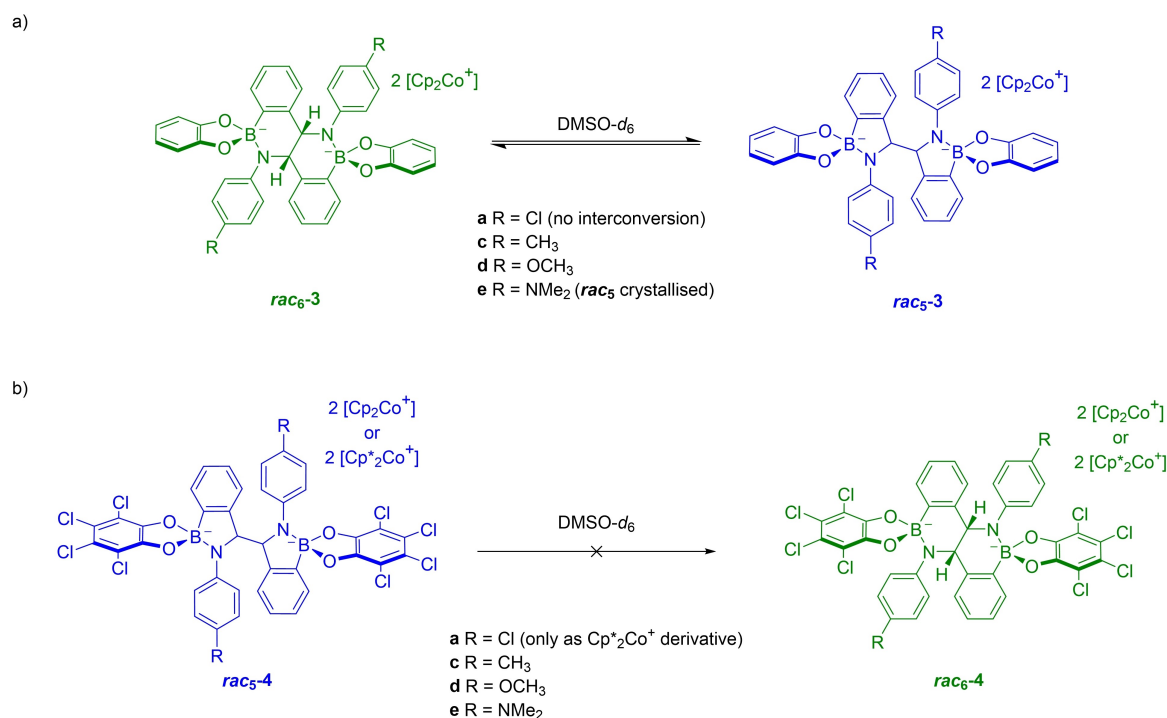


Figure 1. X-ray crystal structures of: a) [*meso*₅-**3a**](Cp₂Co)₂; b) [*rac*₆-**3a**](Cp₂Co)₂; c) [*rac*₅-**4d**](Cp₂Co)₂. For clarity, the Cp₂Co⁺ counteranions and solvent molecules have not been depicted.



Scheme 3. Interconversion between the **rac₅** and **rac₆** isomers upon redissolving crystals of single isomers in DMSO-*d*₆: a) pyrocatechol series; b) tetrachlorocatechol series.

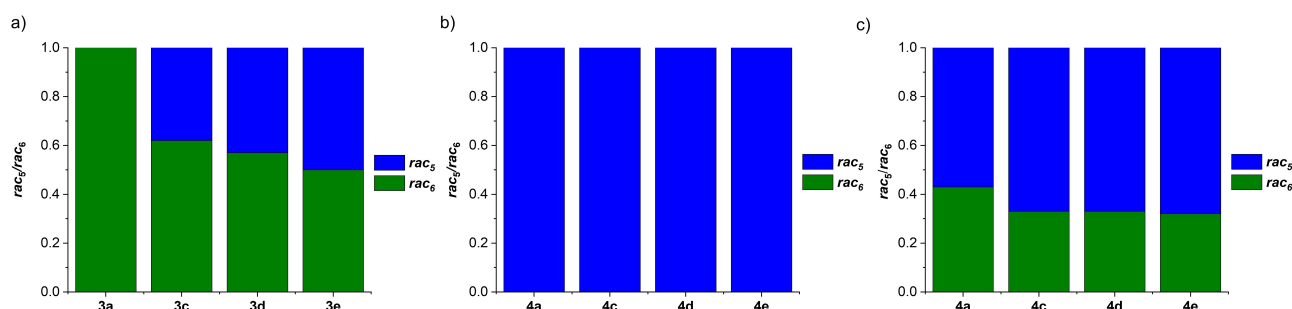


Figure 2. Ratio of **rac₅**/**rac₆** isomers of: a) redissolved **rac-3a,c-e** crystals; b) redissolved **rac-4a,c-e** crystals; c) **rac-4a,c-e** formed from redissolved **rac-3a,c-e** crystals following catechol exchange of pyrocatechol for tetrachlorocatechol.

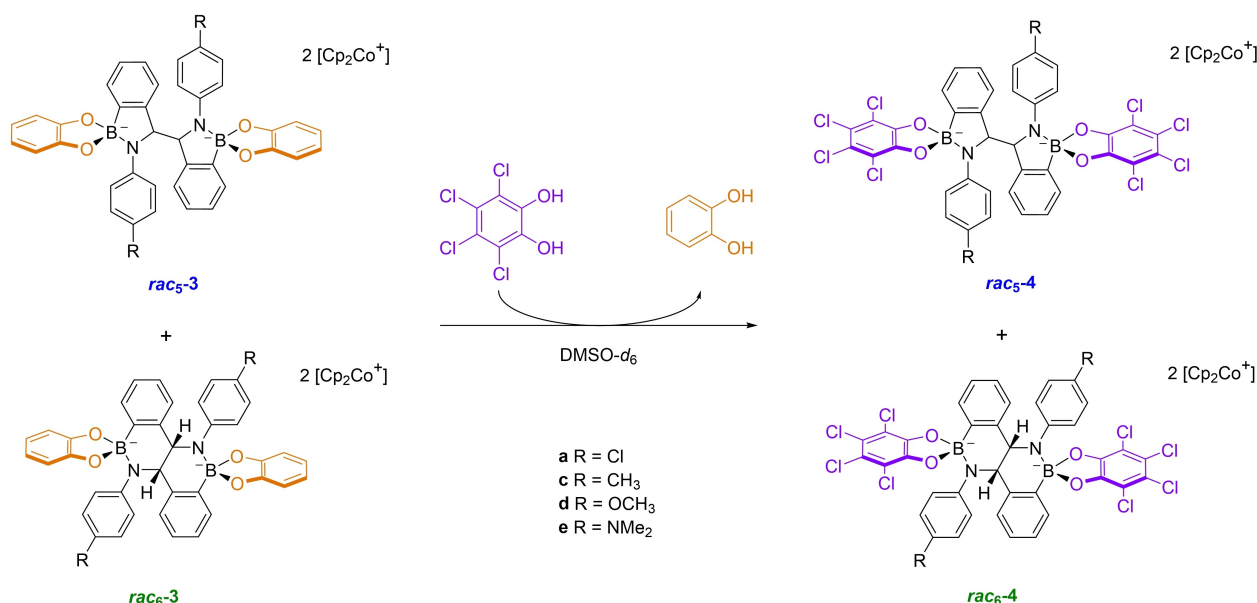
of electron-donating aniline substituents such as OMe and NMe₂. The energetic cost of the rearrangement from the five- to six-membered rings could also account for the lack of interconversion.

Having observed that the catechol component alters the preference for the **rac₅** or **rac₆** isomer, the dynamic nature of the amidoboronates' B–O bonds was investigated via catechol exchange. While catechol exchange has been demonstrated for iminoboronates,^[22c] amidoboronates contain anionic tetrahedral boron centres with filled p-orbitals and this could lower the reactivity towards catechol exchange.^[20d] Nevertheless, Matile and co-workers have reported partial catechol exchange at a tetrahedral boron in boronate esters of benzoboroxoles with water and base.^[14c]

Crystals of individual **rac₅** or **rac₆** isomers were redissolved in DMSO-*d*₆ and equilibrated at room temperature before adding a competing catechol (pyrocatechol or tetrachlorocate-

chol) in portions (Scheme 4 and SI, Section 14). In the case of the pyrocatechol series, the first addition of tetrachlorocatechol led to release of pyrocatechol and the complexity of the NMR spectrum increased in many cases with signals corresponding to the pyrocatechol derivatives decreasing in intensity, while those for the corresponding tetrachlorocatechol derivatives appeared (Figures S139–S142). The presence of additional methine signals suggested the formation of mixed catechol species due to incomplete catechol exchange and therefore, additional portions of tetrachlorocatechol were added where necessary. The signals for the pyrocatechol derivatives disappeared and those belonging to the tetrachlorocatechol derivatives remained, confirming catechol exchange was complete.

In contrast, a control experiment with **rac₅-4d** showed no evidence of catechol exchange upon addition of excess pyrocatechol (Figure S143). This suggests that the tetrachlorocatechol derivative is thermodynamically more stable than the



Scheme 4. Catechol exchange of equilibrated mixtures of $\text{rac}_5\text{-3}$ and $\text{rac}_6\text{-3}$ isomers where tetrachlorocatechol exchanges for pyrocatechol forming a mixture of $\text{rac}_5\text{-4}$ and $\text{rac}_6\text{-4}$. An analogous exchange experiment with $\text{rac}_5\text{-4 d}$ showed no catechol exchange of tetrachlorocatechol for pyrocatechol.

pyrocatechol derivative, attributed to the greater delocalisation of the negative charge with the more electron-withdrawing tetrachlorocatechol.

Comparison of the catechol exchanges within the pyrocatechol series revealed that following catechol exchange with tetrachlorocatechol, both the $\text{rac}_5\text{-4}$ and $\text{rac}_6\text{-4}$ isomers are present (Figure 2c). In contrast, the redissolved $\text{rac}_5\text{-4}$ crystals of the tetrachlorocatechol derivatives did not interconvert into the rac_6 isomer upon equilibration (Figure 2b). We attribute this difference to the existence of an alternative pathway to the rac_6 isomer by catechol exchange rather than via $\text{rac}_5/\text{rac}_6$ interconversion alone; the $\text{rac}_6\text{-3}$ isomer present in the initial mixture can be directly converted to $\text{rac}_6\text{-4}$, the corresponding tetrachlorocatechol derivative.

Conclusion

The scope of the reductive coupling of iminoboronates was expanded to investigate the role of the aniline *para* substituent and catechol on the $\text{rac}_5/\text{rac}_6$ interconversion via dynamic covalent B–N bonds. Amidoboronates based on pyrocatechol crystallised as the rac_6 isomer with the exception of $\text{rac}_5\text{-3 e}$ while those based on tetrachlorocatechol crystallised as the rac_5 isomer regardless of the counteraction. The catechol coarsely tunes the preference for the rac_5 isomer in the tetrachlorocatechol-based amidoboronates since no interconversion to the rac_6 isomer was observed. In contrast, the aniline *para* substituent finely tunes the $\text{rac}_5/\text{rac}_6$ ratio in the pyrocatechol-based amidoboronates with the proportion of $\text{rac}_5\text{-3}$ increasing with more electron-donating aniline substituents.

Catechol exchange experiments demonstrated the dynamic covalent nature of the B–O bonds and the $\text{rac}_5/\text{rac}_6$ ratio was altered upon exchange of pyrocatechol for tetrachlorocatechol with the rac_5 predominating. The rac_6 isomer is proposed to predominantly form via direct conversion of $\text{rac}_6\text{-3}$ to $\text{rac}_6\text{-4}$ by catechol exchange rather than interconversion of $\text{rac}_5\text{-4}$ to $\text{rac}_6\text{-4}$ through the B–N dynamic covalent bonds. Thus, amidoboronates have two types of dynamic covalent bonds that can be exploited to tune the interconversion and resulting distribution between the rac_5 and rac_6 isomers. Exploitation of the B–N and B–O bonds of amidoboronates for more complex dynamic covalent chemistry will be the subject of future investigations.

Acknowledgements

We thank the Deutsche Forschungsgemeinschaft (DFG, project number 447862786) for financial support. We thank Alexandru Sava and Prof. Jonathan Nitschke (University of Cambridge) as well as Michaela Taddey and Anke Sehrer (CAU Kiel) for preliminary studies. We thank the spectroscopy department, Dr. Claus Bier and Johanna Baum for NMR and mass spectral data collection. Open Access funding enabled and organized by Projekt DEAL.

Conflict of Interest

The authors declare no conflict of interest.

Data Availability Statement

The data that support the findings of this study are available in the supplementary material of this article.

Keywords: amidoboronates • dynamic covalent chemistry • radical coupling • rearrangement • supramolecular chemistry

- [1] a) Z. X. Giustra, S.-Y. Liu, *J. Am. Chem. Soc.* **2018**, *140*, 1184–1194; b) C. R. McConnell, S.-Y. Liu, *Chem. Soc. Rev.* **2019**, *48*, 3436–3453; c) M. Hejda, R. Jambor, A. Růžicka, A. Lyčka, L. Dostál, *Dalton Trans.* **2014**, 43, 9012–9015; d) D.-T. Yang, Y. Shi, T. Peng, S. Wang, *Organometallics* **2017**, *36*, 2654–2660; e) H. Noda, Y. Asada, M. Shibasaki, N. Kumagai, *J. Am. Chem. Soc.* **2019**, *141*, 1546–1554; f) J. S. Dhindsa, F. L. Buguis, M. Anghel, J. B. Gilroy, *J. Org. Chem.* **2021**, *86*, 12064–12074; g) D.-T. Yang, J. Zheng, J.-B. Peng, X. Wang, S. Wang, *J. Org. Chem.* **2021**, *86*, 829–836; h) Z. Mo, A. Rit, J. Campos, E. L. Kolychev, S. Aldridge, *J. Am. Chem. Soc.* **2016**, *138*, 3306–3309; i) G. Meng, L. Liu, Z. He, D. Hall, X. Wang, T. Peng, X. Yin, P. Chen, D. Beljonne, Y. Olivier, E. Zysman-Colman, N. Wang, S. Wang, *Chem. Sci.* **2022**, *13*, 1665–1674; j) A. A. Suleymanov, R. Scopelliti, K. Severin, *Inorg. Chem.* **2022**, *61*, 1546–1551; k) J. Full, S. P. Panchal, J. Götz, A.-M. Krause, A. Nowak-Król, *Angew. Chem. Int. Ed.* **2021**, *60*, 4350–4357; *Angew. Chem.* **2021**, *133*, 4396–4403.
- [2] a) D. W. Stephan, *Chem* **2020**, *6*, 1520–1526; b) D. W. Stephan, G. Erker, *Angew. Chem. Int. Ed.* **2010**, *49*, 46–76; *Angew. Chem.* **2010**, *122*, 50–81; c) D. W. Stephan, G. Erker, *Angew. Chem. Int. Ed.* **2015**, *54*, 6400–6441; *Angew. Chem.* **2015**, *127*, 6498–6541.
- [3] a) G. M. Adams, A. L. Colebatch, J. T. Skornia, A. I. McKay, H. C. Johnson, G. C. Lloyd-Jones, S. A. Macgregor, N. A. Beattie, A. S. Weller, *J. Am. Chem. Soc.* **2018**, *140*, 1481–1495; b) D. A. Resendiz-Lara, G. R. Whittell, E. M. Leitao, I. Manners, *Macromolecules* **2019**, *52*, 7052–7064; c) A. L. Colebatch, A. S. Weller, *Chem. Eur. J.* **2019**, *25*, 1379–1390; d) N. E. Stubbs, T. Jurca, E. M. Leitao, C. H. Woodall, I. Manners, *Chem. Commun.* **2013**, 49, 9098–9100.
- [4] a) S. K. Møllerup, S. Wang, *Chem. Soc. Rev.* **2019**, *48*, 3537–3549; b) Q. Hou, L. Liu, S. K. Møllerup, N. Wang, T. Peng, P. Chen, S. Wang, *Org. Lett.* **2018**, *20*, 6467–6470; c) K. Matsui, S. Oda, K. Yoshiura, K. Nakajima, N. Yasuda, T. Hatakeyama, *J. Am. Chem. Soc.* **2018**, *140*, 1195–1198; d) Y. Min, C. Dou, H. Tian, Y. Geng, J. Liu, L. Wang, *Angew. Chem. Int. Ed.* **2018**, *57*, 2000–2004; *Angew. Chem.* **2018**, *130*, 2018–2022.
- [5] a) F. Vidal, H. Lin, C. Morales, F. Jäkle, *Molecules* **2018**, *23*, 405; b) C. Bao, Y.-J. Jiang, H. Zhang, X. Lu, J. Sun, *Adv. Funct. Mater.* **2018**, *28*, 1800560.
- [6] C. R. Opie, H. Noda, M. Shibasaki, N. Kumagai, *Chem. Eur. J.* **2019**, *25*, 4648–4653.
- [7] a) U. Gellrich, *Angew. Chem. Int. Ed.* **2018**, *57*, 4779–4782; *Angew. Chem.* **2018**, *130*, 4869–4872; b) M. Hasenbeck, S. Ahles, A. Averdunk, J. Becker, U. Gellrich, *Angew. Chem. Int. Ed.* **2020**, *59*, 23885–23891; *Angew. Chem.* **2020**, *132*, 24095–24101; c) M. A. Dureen, D. W. Stephan, *J. Am. Chem. Soc.* **2010**, *132*, 13559–13568; d) J. Guo, O. Cheong, K. L. Bamford, J. Zhou, D. W. Stephan, *Chem. Commun.* **2020**, *56*, 1855–1858; e) T. Wang, C. G. Daniliuc, C. Mück-Lichtenfeld, G. Kehr, *J. Am. Chem. Soc.* **2018**, *140*, 3635–3643; f) M.-A. Courtemanche, A. P. Pulis, É. Rochette, M.-A. Légaré, D. W. Stephan, F.-G. Fontaine, *Chem. Commun.* **2015**, *51*, 9797–9800.
- [8] a) Y. Jin, C. Yu, R. J. Denman, W. Zhang, *Chem. Soc. Rev.* **2013**, *42*, 6634–6654; b) S. J. Rowan, S. J. Cantrill, G. R. L. Cousins, J. K. M. Sanders, J. F. Stoddart, *Angew. Chem. Int. Ed.* **2002**, *41*, 898–952; *Angew. Chem.* **2002**, *114*, 938–993; c) S. Chatterjee, E. V. Anslyn, A. Bandyopadhyay, *Chem. Sci.* **2021**, *12*, 1585–1599; d) R.-C. Brachvogel, M. von Delius, *Eur. J. Org. Chem.* **2016**, *2016*, 3662–3670; e) F. Beuerle, B. Gole, *Angew. Chem. Int. Ed.* **2018**, *57*, 4850–4878; *Angew. Chem.* **2018**, *130*, 4942–4972.
- [9] a) X. Wang, O. Shyshov, M. Hanževački, C. M. Jäger, M. von Delius, *J. Am. Chem. Soc.* **2019**, *141*, 8868–8876; b) O. Shyshov, R.-C. Brachvogel, T. Bachmann, R. Srikantharajah, D. Segets, F. Hampel, R. Puchta, M. von Delius, *Angew. Chem.* **2017**, *129*, 794–799; *Angew. Chem. Int. Ed.* **2017**, *56*, 776–781; c) S. Yang, D. Larsen, M. Pellegrini, S. Meier, D. F. Mierke, S. R. Beeren, I. Aprahamian, *Chem* **2021**, *7*, 2190–2200; d) D. Larsen, S. R. Beeren, *Chem. Sci.* **2019**, *10*, 9981–9987; e) B. M. Matysiak, P. Nowak, I. Cvrtila, C. G. Pappas, B. Liu, D. Komáromy, S. Otto, *J. Am. Chem. Soc.* **2017**, *139*, 6744–6751; f) C. G. Pappas, P. K. Mandal, B. Liu, B. Kauffmann, X. Miao, D. Komáromy, W. Hoffmann, C. Manz, R. Chang, K. Liu, K. Pagel, I. Huc, S. Otto, *Nat. Chem.* **2020**, *12*, 1180–1186; g) A. S. Bhat, S. M. Elbert, W.-S. Zhang, F. Rominger, M. Dieckmann, R. R. Schröder, M. Mastalerz, *Angew. Chem. Int. Ed.* **2019**, *58*, 8819–8823; *Angew. Chem.* **2019**, *131*, 8911–8915; h) M. Hählsler, M. Mastalerz, *Chem. Eur. J.* **2021**, *27*, 233–237; i) T. H. G. Schick, J. C. Lauer, F. Rominger, M. Mastalerz, *Angew. Chem. Int. Ed.* **2019**, *58*, 1768–1773; *Angew. Chem.* **2019**, *131*, 1782–1787; j) N. Schäfer, M. Bühler, L. Heyer, M. I. S. Röhr, F. Beuerle, *Chem. Eur. J.* **2021**, *27*, 6077–6085; k) S. Ivanova, E. Köster, J. J. Holstein, N. Keller, G. H. Clever, T. Bein, F. Beuerle, *Angew. Chem. Int. Ed.* **2021**, *60*, 17455–17463; l) K. Ono, S. Shimo, K. Takahashi, N. Yasuda, H. Uekusa, N. Iwasawa, *Angew. Chem. Int. Ed.* **2018**, *57*, 3113–3117; *Angew. Chem.* **2018**, *130*, 3167–3171; m) M. Kołodziejewski, A. R. Stefankiewicz, J.-M. Lehn, *Chem. Sci.* **2019**, *10*, 1836–1843.
- [10] a) B. Akgun, D. G. Hall, *Angew. Chem. Int. Ed.* **2016**, *55*, 3909–3913; *Angew. Chem.* **2016**, *128*, 3977–3981; b) S. Ulrich, *Acc. Chem. Res.* **2019**, *52*, 510–519.
- [11] O. R. Cromwell, J. Chung, Z. Guan, *J. Am. Chem. Soc.* **2015**, *137*, 6492–6495.
- [12] a) W. A. Ogden, Z. Guan, *J. Am. Chem. Soc.* **2018**, *140*, 6217–6220; b) M. Röttger, T. Domenech, R. van der Weegen, A. Breuillac, R. Nicolaÿ, L. Leibler, *Science* **2017**, *356*, 62–65.
- [13] a) N. Luisier, K. Schenk, K. Severin, *Chem. Commun.* **2014**, *50*, 10233–10236; b) M. E. Smithmyer, C. C. Deng, S. E. Cassel, P. J. LeValley, B. S. Sumerlin, A. M. Kloxin, *ACS Macro Lett.* **2018**, *7*, 1105–1110.
- [14] a) S. P. Black, J. K. M. Sanders, A. R. Stefankiewicz, *Chem. Soc. Rev.* **2014**, *43*, 1861–1872; b) B. Balakrishna, A. Menon, K. Cao, S. Gsänger, S. B. Beil, J. Villalva, O. Shyshov, O. Martin, A. Hirsch, B. Meyer, U. Kaiser, D. M. Guldi, M. von Delius, *Angew. Chem. Int. Ed.* **2020**, *59*, 18774–18785; *Angew. Chem.* **2020**, *132*, 18933–18945; c) S. Lascano, K.-D. Zhang, R. Wehlauch, K. Gademann, N. Sakai, S. Matile, *Chem. Sci.* **2016**, *7*, 4720–4724.
- [15] a) Q. Ji, O. Š. Miljanić, *J. Org. Chem.* **2013**, *78*, 12710–12716; b) G. Kaiser, J. K. M. Sanders, *Chem. Commun.* **2000**, 1763–1764.
- [16] B. Fuchs, A. Nelson, A. Star, J. F. Stoddart, S. Vidal, *Angew. Chem. Int. Ed.* **2003**, *42*, 4220–4224; *Angew. Chem.* **2003**, *115*, 4352–4356.
- [17] a) D. Hartmann, T. Thorwart, R. Müller, J. Thusek, J. Schwabedissen, A. Mix, J.-H. Lamm, B. Neumann, N. W. Mitzel, L. Greb, *J. Am. Chem. Soc.* **2021**, *143*, 18784–18793; b) D. Hartmann, L. Greb, *Angew. Chem. Int. Ed.* **2020**, *59*, 22510–22513; *Angew. Chem.* **2020**, *132*, 22699–22702; c) J. Roesser, D. Prill, M. J. Bojdys, P. Fayon, A. Trewin, A. N. Fitch, M. U. Schmidt, A. Thomas, *Nat. Chem.* **2017**, *9*, 977–982.
- [18] G. Men, J.-M. Lehn, *Chem. Sci.* **2019**, *10*, 90–98.
- [19] a) R. Gu, J.-M. Lehn, *J. Am. Chem. Soc.* **2021**, *143*, 14136–14146; b) D. He, R. Clowes, M. A. Little, M. Liu, A. I. Cooper, *Chem. Commun.* **2021**, *57*, 6141–6144; c) A. Kai, B. D. Egleston, A. Tarzia, R. Clowes, M. E. Briggs, K. E. Jelfs, A. I. Cooper, R. L. Greenaway, *Adv. Funct. Mater.* **2021**, *31*, 2106116; d) F. Schaufelberger, K. Seigel, O. Ramström, *Chem. Eur. J.* **2020**, *26*, 15581–15588; e) V. Abet, F. T. Szczypiński, M. A. Little, V. Santolini, C. D. Jones, R. Evans, C. Wilson, X. Wu, M. F. Thorne, M. J. Bennisson, P. Cui, A. I. Cooper, K. E. Jelfs, A. G. Slater, *Angew. Chem. Int. Ed.* **2020**, *59*, 16755–16763; *Angew. Chem.* **2020**, *132*, 16898–16906.
- [20] a) S. D. Bull, M. G. Davidson, J. M. H. van den Elsen, J. S. Fossey, A. T. A. Jenkins, Y.-B. Jiang, Y. Kubo, F. Marken, K. Sakurai, J. Zhao, T. D. James, *Acc. Chem. Res.* **2013**, *46*, 312–326; b) X. Sun, B. M. Chapin, P. Metola, B. Collins, B. Wang, T. D. James, E. V. Anslyn, *Nat. Chem.* **2019**, *11*, 768–778; c) L. Zhu, S. H. Shabbir, M. Gray, V. M. Lynch, S. Sorey, E. V. Anslyn, *J. Am. Chem. Soc.* **2006**, *128*, 1222–1232; d) B. Marco-Dufort, R. Iten, M. W. Tibbitt, *J. Am. Chem. Soc.* **2020**, *142*, 15371–15385; e) E. Giraldo, R. Scopelliti, F. Fadaei-Tirani, K. Severin, *Inorg. Chem.* **2021**, *60*, 10873–10879.
- [21] S. Delpierre, B. Willocq, J. De Winter, P. Dubois, P. Gerbaux, J.-M. Raquez, *Chem. Eur. J.* **2017**, *23*, 6730–6735.
- [22] a) H. E. Dunn, J. C. Catlin, H. R. Snyder, *J. Org. Chem.* **1968**, *33*, 4483–4486; b) A. M. Kelly, Y. Pérez-Fuertes, S. Arimori, S. D. Bull, T. D. James, *Org. Lett.* **2006**, *8*, 1971–1974; c) M. Hutin, G. Bernardinelli, J. R. Nitschke, *Chem. Eur. J.* **2008**, *14*, 4585–4593.
- [23] a) E. G. Shcherbakova, T. Minami, V. Brega, T. D. James, P. Anzenbacher, *Angew. Chem. Int. Ed.* **2015**, *54*, 7130–7133; *Angew. Chem.* **2015**, *127*, 7236–7239; b) E. G. Shcherbakova, V. Brega, V. M. Lynch, T. D. James, P. Anzenbacher, *Chem. Eur. J.* **2017**, *23*, 10222–10229.
- [24] S. Delpierre, B. Willocq, G. Manini, V. Lemaury, J. Goole, P. Gerbaux, J. Cornil, P. Dubois, J.-M. Raquez, *Chem. Mater.* **2019**, *31*, 3736–3744.
- [25] a) A. Bandyopadhyay, J. Gao, *Chem. Eur. J.* **2015**, *21*, 14748–14752; b) R. Russo, R. Padanah, F. Fernandes, L. F. Veiros, F. Corzana, P. M. P. Gois, *Chem. Eur. J.* **2020**, *26*, 15226–15231; c) P. M. S. Cal, J. B. Vicente, E.

- Pires, A. V. Coelho, L. F. Veiros, C. Cordeiro, P. M. P. Gois, *J. Am. Chem. Soc.* **2012**, *134*, 10299–10305; d) H. Faustino, M. J. S. A. Silva, L. F. Veiros, G. J. L. Bernardes, P. M. P. Gois, *Chem. Sci.* **2016**, *7*, 5052–5058; e) A. J. van der Zouwen, A. Jeucken, R. Steneker, K. F. Hohmann, J. Lohse, D. J. Slotboom, M. D. Witte, *Chem. Eur. J.* **2021**, *27*, 3292–3296.
- [26] a) R. Ma, C. Zhang, Y. Liu, C. Li, Y. Xu, B. Li, Y. Zhang, Y. An, L. Shi, *RSC Adv.* **2017**, *7*, 21328–21335; b) Y. Li, Y. Liu, R. Ma, Y. Xu, Y. Zhang, B. Li, Y. An, L. Shi, *ACS Appl. Mater. Interfaces* **2017**, *9*, 13056–13067; c) A. Biswas, T. Ghosh, P. K. Gavel, A. K. Das, *ACS Appl. Bio Mater.* **2020**, *3*, 1052–1060; d) R. Cheng, G. Li, L. Fan, J. Jiang, Y. Zhao, *Chem. Commun.* **2020**, *56*, 12246–12249.
- [27] E. N. Keyzer, A. Sava, T. K. Ronson, J. R. Nitschke, A. J. McConnell, *Chem. Eur. J.* **2018**, *24*, 12000–12005.
- [28] C. Hansch, A. Leo, R. W. Taft, *Chem. Rev.* **1991**, *91*, 165–195.
- [29] Deposition Numbers 2141398 (for **1a**), 2141391 (for **1d**), 2141393 (for **1e**), 2141397 (for **2d**), 2141396 (for [**meso**₅-**3a**](Cp₂Co⁺)₂), 2141394 (for [**rac**₆-**3a**](Cp₂Co⁺)₂), 2141395 (for [**rac**₅-**4a**](Cp^{*}₂Co⁺)₂), 2141390 (for [**rac**₅-**4d**](Cp₂Co⁺)₂), 2141389 (for [**rac**₅-**4e**](Cp₂Co⁺)₂), 2141392 (for [**rac**₅-**4e**](Cp^{*}₂Co⁺)₂) contain the supplementary crystallographic data for this paper. These data are provided free of charge by the joint Cambridge Crystallographic Data Centre and Fachinformationszentrum Karlsruhe Access Structures service www.ccdc.cam.ac.uk/structures.
- [30] a) Y. Liu, H. Yi, T. Tao, P. Hoa, C. Chunyan, *Angew. Chem. Int. Ed.* **2018**, *57*, 9023–9027; *Angew. Chem.* **2018**, *130*, 9161–9165; b) K. Oda, S. Hiroto, H. Shinokubo, *J. Mater. Chem. C* **2017**, *5*, 5310–5315.
- [31] A small quantity of **meso**₅-**3a** also crystallised from the reaction mixture and was present in the NMR spectra of the redissolved **rac**₆-**3a** crystals.
- [32] While both **meso**₅-**3b** and **rac**₆-**3b** are known to crystallise from the reaction mixture (see ref. [27]), only **meso**₅-**3b** crystals were obtained.

Manuscript received: January 25, 2022

Revised manuscript received: February 7, 2022

Accepted manuscript online: February 8, 2022